

Note

An Accelerated Computing Technique for Steady Fluid Flows

1. INTRODUCTION

A number of numerical methods for solving the incompressible Navier-Stokes equations have been presented and many studies have been made of the two- or three-dimensional viscous fluid flows [1-9]. In respect to differencing technique, there are the implicit scheme such as the ADI method [1] and the explicit scheme such as the MAC method [2]. For the large geometry problems, the former has a disadvantageous restriction on the length of matrix elements and the latter requires a large computing time.

Recently, there has been a growing need for the application to steady fluid flow problems in the complicated and large geometry such as a wire-spaced fuel pin bundle flow in connection to the detailed hot spot temperature analyses, where the cell size in the principal flow direction is usually set to be several times of the cell sizes in the transverse flow directions [10, 11].

In case of the steady flow problems, it is reported by Hirt [9] that it is possible to speed up the asymptotic attainment of steady flow by setting the mass convergence criterion to be less severe. Patankar and Spalding [6] have presented a numerical method for the steady three-dimensional viscous flow with one primary flow direction by a parabolic flow approximation.

However, in the usual method the pressure and mass convergence is slow when the cell size in the principal flow direction is large compared to the cell sizes in the transverse flow direction.

In this note, an accelerated computing technique is presented for solving the steady flow problems. The technique presented here is a slightly modified type of Hirt and Cook's method [5] (hereafter referred to the SOLA method) based on Harlow and Welch (so-called MAC method) [2]. The essence of this technique consists in introducing directional velocity-correction factors and cell boundary condition parameters to achieve the mass conservation in a considerably small number of pressure iterations.

In order to demonstrate the effectiveness of this technique, its performance is compared with that of the SOLA method for a three-dimensional steady flow problem within a duct with an internal obstacle.

2. TECHNIQUE

2.1. Basic Equations

The SOLA method, which is a simplified version of the MAC method, is a technique for solving the time-dependent Eulerian equations of momentum conservation and the mass conservation.

First, the time advanced velocity components ($u_{i,j,k}^{n+1}$, $v_{i,j,k}^{n+1}$, $w_{i,j,k}^{n+1}$) are calculated from the differential equations of momentum conservation approximated by the forward differencing with respect to time and a combination of the central and the upstream differencing with respect to space. Superscript n is used for the time level at which quantities are evaluated and subscripts i, j and k denote the cell location in x , y and z directions, respectively.

Second, the pressure field $p_{i,j,k}^{n+1}$ is simultaneously determined such that the time advanced velocity components obtained from the first step satisfy the mass conservation equation by introducing the relaxation parameter $\Delta\tau_{i,j,k}$ and the following iteration formulae for the $l+1$ iteration:

$$(p_{i,j,k}^{n+1})^{l+1} = (p_{i,j,k}^{n+1})^l + (\delta p_{i,j,k}^{n+1})^l, \quad (1a)$$

$$(\delta p_{i,j,k}^{n+1})^l = -\Delta\tau_{i,j,k}(\nabla \cdot v_{i,j,k}^{n+1})^l. \quad (1b)$$

The velocity components are adjusted to reflect this pressure change as follows:

$$(u_{i+\xi,j,k}^{n+1})^{l+1} = (u_{i+\xi,j,k}^{n+1})^l \pm C_x \left(\frac{\delta t}{\rho \delta x} \right) (\delta P_{i,j,k}^{n+1})^l \cdot \gamma_{i+\xi,j,k}, \quad (2a)$$

$$(v_{i,j+\xi,k}^{n+1})^{l+1} = (v_{i,j+\xi,k}^{n+1})^l \pm C_y \left(\frac{\delta t}{\rho \delta y} \right) (\delta P_{i,j,k}^{n+1})^l \cdot \gamma_{i,j+\xi,k}, \quad (2b)$$

$$(w_{i,j,k+\xi}^{n+1})^{l+1} = (w_{i,j,k+\xi}^{n+1})^l \pm C_z \left(\frac{\delta t}{\rho \delta z} \right) (\delta P_{i,j,k}^{n+1})^l \cdot \gamma_{i,j,k+\xi}; \quad (2c)$$

here ξ is 0 or -1 and ζ is defined such that:

$$\text{if } \xi = 0, \quad \zeta = +1,$$

$$\text{if } \xi = -1, \quad \zeta = -1.$$

In Eq. (2), ρ is the fluid density, δt is the time increment, and δx , δy and δz are the space increments in the x , y and z directions, respectively. The relaxation parameter $\Delta\tau_{i,j,k}$ is determined such that above updated velocity divergence vanishes as follows:

$$\Delta\tau_{i,j,k} = \omega(\rho/\delta t A), \quad (3a)$$

$$A \equiv \frac{C_x}{\delta x^2} (\gamma_{i+1,j,k} + \gamma_{i-1,j,k}) + \frac{C_y}{\delta y^2} (\gamma_{i,j+1,k} + \gamma_{i,j-1,k}) \\ + \frac{C_z}{\delta z^2} (\gamma_{i,j,k+1} + \gamma_{i,j,k-1}), \quad (3b)$$

where ω is an accelerating factor explained in the next section. $\gamma_{i,j,k}$'s are the cell boundary condition parameters, which are 1 for a fluid cell (i,j,k) and 0 for boundary cells. By introducing these parameters, the cell pressure can be suitably corrected in such a way as to directly reflect the boundary condition for the normal velocity component in each mass continuity iteration, while in the SOLA method the cell pressure is so adjusted one step later than the each iteration as to reflect the boundary condition. For this reason, the $\gamma_{i,j,k}$ cell boundary condition application is effective in speeding the iterative convergence. When $\gamma_{i,j,k}$'s are all unity, Eq. (3) corresponds to Eq. (6) in reference [5], in which all cell pressures are adjusted by the same relaxation parameter.

C_x , C_y and C_z in Eq. (3) are the velocity-correction factors (referred to C factors in abbreviation) introduced in this note. The usual method corresponds to $\{C_x = C_y = C_z = 1\}$. In the usual method the pressure and mass convergence is slow when the cell size in the principal flow direction is large compared to the cell size in the transverse direction. When the transverse cell size is small the relaxation parameter is small as can be seen from Eq. (3). Thus, it is underrelaxing variations in the principal flow direction. Namely, in the usual method the relaxation factor is limited by the smallest cell size, and contains no information regarding direction for the principal pressure variation. The introduction of the velocity-correction factors inserts this information into the relaxation parameter. One-dimensional flow in a long pipe can be considered as a useful limiting case. If the radial zone sizes are small compared to their axial lengths the iteration will be severely limited, even though no radial pressure variation exists in the final answer. Letting the axial C factor approach infinity in this case reduces the problem to one-dimensional axial flow as desired. This is a simple example to show why the introduction of C factors has merit.

2.2. Stability and Convergence Rate

Introduction of the velocity-correction factors yields the following discrete Poisson equation for the pressure which corresponds to the equation derived by Viecegli [4]:

$$\begin{aligned}
 (P_{i,j,k}^{n+1})^{l+1} = & (P_{i,j,k}^{n+1})^l \\
 & + \left(\frac{\Delta\tau \delta t}{\rho}\right) \left(\frac{C_x}{\delta x^2}\right) [(P_{i+1,j,k}^{n+1})^l - 2(P_{i,j,k}^{n+1})^l + (P_{i-1,j,k}^{n+1})^{l+1}] \\
 & + \left(\frac{\Delta\tau \delta t}{\rho}\right) \left(\frac{C_y}{\delta y^2}\right) [(P_{i,j+1,k}^{n+1})^l - 2(P_{i,j,k}^{n+1})^l + (P_{i,j-1,k}^{n+1})^{l+1}] \\
 & + \left(\frac{\Delta\tau \delta t}{\rho}\right) \left(\frac{C_z}{\delta z^2}\right) [(P_{i,j,k+1}^{n+1})^l - 2(P_{i,j,k}^{n+1})^l + (P_{i,j,k-1}^{n+1})^{l+1}] \\
 & + \nabla\tau \cdot S_{i,j,k}^n, \tag{4}
 \end{aligned}$$

where $S_{i,j,k}^n$ is a source function in terms of the old velocity, advection, viscosity and body force. In Eq. (4), the pressure of the cells $(i-1, j, k)$, $(i, j-1, k)$ and $(i, j, k-1)$ is replaced with the latest values at the $(l+1)$ th iteration while sweeping in the direction of increasing i, j and k in use of the successive over relaxation method.

Based on a von Neuman stability theory, the amplification factor $|G(\theta_x, \theta_y, \theta_z)|$ (referred to $|G|$ factor in abbreviation) defined as Eq. (5a) is given by Eq. (5b) in inner region:

$$|G(\theta_x, \theta_y, \theta_z)| \equiv \frac{|(V(\theta_x, \theta_y, \theta_z))^{l+1}|}{|(V(\theta_x, \theta_y, \theta_z))^l|} \quad (5a)$$

$$= \frac{g(\theta_x, \theta_y, \theta_z)}{f(\theta_x, \theta_y, \theta_z)}, \quad (5b)$$

where

$$\begin{aligned} g(\theta_x, \theta_y, \theta_z) &\equiv \left\{ 1 - 2\alpha \left(\frac{C_x}{\delta x^2} + \frac{C_y}{\delta y^2} + \frac{C_z}{\delta z^2} \right) \right\}^2 + 2\alpha \left\{ 1 - 2\alpha \left(\frac{C_x}{\delta x^2} + \frac{C_y}{\delta y^2} + \frac{C_z}{\delta z^2} \right) \right\} \\ &\cdot \left\{ \frac{C_x \cos \theta_x}{\delta x^2} + \frac{C_y \cos \theta_y}{\delta y^2} + \frac{C_z \cos \theta_z}{\delta z^2} \right\} + \alpha^2 \left\{ \left(\frac{C_x}{\delta x^2} \right)^2 + \left(\frac{C_y}{\delta y^2} \right)^2 + \left(\frac{C_z}{\delta z^2} \right)^2 \right. \\ &\left. + 2 \frac{C_x C_y}{\delta x^2 \delta y^2} \cos(\theta_x - \theta_y) + 2 \frac{C_y C_z}{\delta y^2 \delta z^2} \cos(\theta_y - \theta_z) + 2 \frac{C_z C_x}{\delta z^2 \delta x^2} \cos(\theta_z - \theta_x) \right\}, \end{aligned}$$

$f(\theta_x, \theta_y, \theta_z)$

$$\begin{aligned} &\equiv \left\{ 1 - 2\alpha \left(\frac{C_x \cos \theta_x}{\delta x^2} + \frac{C_y \cos \theta_y}{\delta y^2} + \frac{C_z \cos \theta_z}{\delta z^2} \right) \right. \\ &\left. + \alpha^2 \left\{ \left(\frac{C_x}{\delta x^2} \right)^2 + \left(\frac{C_y}{\delta y^2} \right)^2 + \left(\frac{C_z}{\delta z^2} \right)^2 \right. \right. \\ &\left. \left. + 2 \frac{C_x C_y}{\delta x^2 \delta y^2} \cos(\theta_x - \theta_y) + 2 \frac{C_y C_z}{\delta y^2 \delta z^2} \cos(\theta_y - \theta_z) + 2 \frac{C_z C_x}{\delta z^2 \delta x^2} \cos(\theta_z - \theta_x) \right\} \right\}, \end{aligned}$$

with $\alpha = \Delta t \delta t / \rho$. In Eq. (5a), θ_x, θ_y and θ_z are x, y and z components of phase angle in Fourier series, and $(V(\theta_x, \theta_y, \theta_z))^l$ and $(V(\theta_x, \theta_y, \theta_z))^{l+1}$ are the amplitude of the Fourier component corresponding to the phase angle $(\theta_x, \theta_y, \theta_z)$ at the l th and $(l+1)$ th iteration, respectively. $|G|$ factor depends on space increment ratios $(\delta y/\delta x, \delta z/\delta x)$ and C factor ratios $(C_y/C_x, C_z/C_x)$. For $|G(\theta_x, \theta_y, \theta_z)| < 1$, the Fourier components diminish with increasing l . The smaller the amplification factor, the faster the convergence of the numerical solution. The inequality $|G(\theta_x, \theta_y, \theta_z)| < 1$ leads to $\omega < 2$ for all phase angles. It is usually safe to assume that the optimum value of ω for most rapid convergence occurs fairly close to the stability limit and to start calculations with ω at about $0.9 \omega_{\max}$ [4].

Now we will consider the dependence of the convergence rate on the C factors. As mentioned in the Introduction, the cell size δz in the principal flow direction is usually large compared to the cell sizes in the transverse flow directions in fuel pin bundle flow analyses. Hence the dependence of $|G|$ factor on C_z factor has been examined numerically by using a computer for the case $\{\delta x : \delta y : \delta z = 1 : 1 : 5\}$ with $\omega = 1.8$ in $(4 \times 4 \times 7)$ cells and $(12 \times 12 \times 12)$ cells including boundary cells. The result has shown that the amplification factor $|G|$ is a concave function with respect to C_z for many phase angles except for some cases where $|G|$ is a very gradually increasing function, the values of which are, of course, less than 1 for all C_z values. According to Frankel [12], the convergence rate of the Fourier component with the minimum or maximum wave number is most slow. The present results have shown that the amplification factors with the minimum wave numbers for x and y components (corresponding to $(\theta_x = \theta_y = \pi/10)$ for $(12 \times 12 \times 12)$ cells) and with the maximum wave numbers for x and y components (corresponding to $(\theta_x = \theta_y = \pi)$ for $(12 \times 12 \times 12)$ cells) are both concave functions for all θ_z values with respect to C_z values such as $C_z \geq 1$, as shown in Fig. 1 for the case of $(12 \times 12 \times 12)$ cells.

The optimum values of C factors for most rapid convergence strongly depend on the cell size ratios but weekly depend on the number of cells according to my numerical experience. Therefore, in practical application, we have only to find the optimum values at the first time cycle for a small number of cells by means of survey

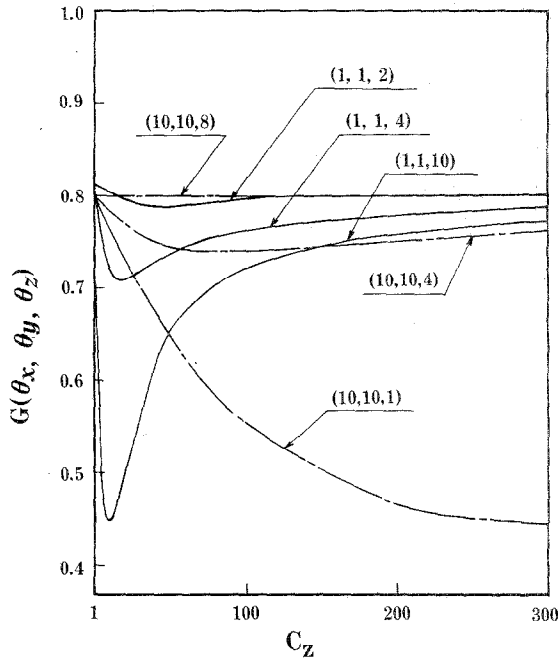


FIG. 1. Dependency of amplification factor $|G(\theta_x, \theta_y, \theta_z)|$ on C_z factor. The numbers in parenthesis (n_x, n_y, n_z) are defined as $(\theta_x = (\pi/10) n_x, \theta_y = (\pi/10) n_y, \theta_z = (\pi/10) n_z)$.

calculation on C factors under the same cell size ratios as those of large geometry, and those optimum values can also be used for the large number of cells without much loss of the merit in use of C factors.

3. TEST CALCULATIONS AND RESULTS

To demonstrate the effectiveness of this technique, test calculations on a square cross-sectional duct flow with an internal obstacle were carried out. A cartesian mesh is used that is the same as the $(4 \times 4 \times 7)$ cells used in the previous section with $\delta x = 10$ cm. An internal obstacle region is defined at the cell $(i = 2, j = 2, k = 4)$. The non-slip condition on the wall and the continuative outflow condition are imposed. The mass convergence criterion is 10^{-3} /sec. The primary flow direction corresponds to the z direction and the inlet velocity $w_{i,j,1}$ is 5 m/sec. For this test calculation, the optimum value of C_z was about 200 with $C_x = C_y = 1$ as determined from survey calculations.

At every time cycle over the beginning 5 cycles, iteration numbers required in the mass convergence calculations are shown in Table I, in which the cases A, B and C correspond to $\{C_x = 1, C_y = 1, C_z = 1\}$ with no use of $\gamma_{i,j,k}$, $\{C_x = 1, C_y = 1, C_z = 200\}$ with no use of $\gamma_{i,j,k}$ and $\{C_x = 1, C_y = 1, C_z = 200\}$ with $\gamma_{i,j,k}$, respectively. At the first time cycle, the case B required an iteration number of 81 which is about 1/50 of that required in the case A. The iteration number for the case C is further decreased to about 1/2 of that for the case B.

After 55 cycles of time advancement, almost steady flow solutions were obtained. At this time cycle, fluid velocity components ($w_{3,3,4}$, $w_{2,2,5}$, $u_{2,2,5}$) of typical cells and their normalized deviations from those of the case A are shown in Table II, where $w_{3,3,4}$, $w_{2,2,5}$ and $u_{2,2,5}$ correspond to the maximum primary component, the

TABLE I
Iteration Numbers Required in the Mass Convergence Calculations

Cycle no. of time	Iteration number		
	Case A	Case B	Case C
1	3931	81	43
2	3543	64	34
3	896	45	27
4	663	39	24
5	575	33	22

TABLE II
Velocity Components of Typical Cells
and Normalized Deviations from Those of Case A

Velocity and deviation ^a	Case A	Case B	Case B'
$w_{3,3,4}$ (m/sec)	7.29318	7.30151	7.29764
$\frac{w_{3,3,4} - a}{a}$ (%)	0	0.114	6.12×10^{-2}
$\frac{w_{3,3,4} - a}{\langle w_4 \rangle}$ (%)	0	0.125	8.92×10^{-2}
$w_{2,2,5}$ (m/sec)	1.88793	1.89690	1.89069
$\frac{w_{2,2,5} - b}{b}$ (%)	0	0.475	0.146
$\frac{w_{2,2,5} - b}{\langle w_5 \rangle}$ (%)	0	0.179	5.52×10^{-2}
$u_{2,2,5}$ (m/sec)	-0.188832	-0.189694	-0.189044
$\frac{u_{2,2,5} - c}{c}$ (%)	0	-0.456	-0.112
$\frac{u_{2,2,5} - c}{\langle w_5 \rangle}$ (%)	0	-1.72×10^{-2}	-4.24×10^{-3}

^a a , b and c correspond to $w_{3,3,4}$, $w_{2,2,5}$ and $u_{2,2,5}$ calculated in the case A, respectively. $\langle w_k \rangle$ is the bulk mean velocity at k in the z direction, that is, $\langle w_4 \rangle = 6.67$ m/sec and $\langle w_5 \rangle = 5$ m/sec.

minimum primary component and the maximum secondary component of velocity, respectively. In the case B', after 50 cycles of time advancement under $\{C_x = 1, C_y = 1, C_z = 200\}$, the time advancement calculations were continued until 55 cycles of time with $\{C_x = 1, C_y = 1, C_z = 1\}$. The deviations of $w_{3,3,4}$ from that of the case A are about 0.1% in the case B and about 0.06% in the case B'. The normalized deviations of $w_{2,2,5}$ to that of the case A are 0.475% in the case B and 0.146% in the case B' but those deviations to the bulk mean velocity are 0.179% in the case B and 5.52×10^{-2} % in the case B. The normalized deviations of $u_{2,2,5}$ to that of the case A are -0.456% in the case B and -0.112% in the case B' but to the bulk mean velocity negligible small in both cases. Little difference in the converged solutions between case A and case B is seen in Table II. The reason for this is that the first guess for the velocities, at the beginning of each cycle and before the pressure iteration, contains the correct pressure gradient terms. The modified iteration is only used to adjust pressures to insure mass continuity. When steady state convergence is obtained the first guess for the velocities is the correct steady state result.

ACKNOWLEDGMENTS

The author wishes to express his gratitude to Dr. H. Hishida and Mr. Y. Yamashita of MAPI for their helpful discussions.

REFERENCES

1. C. E. PEARSON, *J. Fluid Mech.* **21-4** (1965), 611.
2. F. H. HARLOW AND J. E. WELCH, *Phys. Fluids* **8** (1965), 2182.
3. A. J. CHORIN, *Math. Comp.* **22** (1968), 745.
4. J. A. VIECELLI, *J. Comput. Phys.* **8** (1971), 119.
5. C. W. HIRT AND J. L. COOK, *J. Comput. Phys.* **10** (1971), 324.
6. S. V. PATANKAR AND D. B. SPALDING, *Int. J. Heat Mass Transfer* **15** (1972), 1787.
7. W. R. BRILEY, *J. Comput.* **14** (1974), 8.
8. C. W. HIRT, B. D. NICHOLS, AND N. C. ROMERO, Los Alamos Report LA-5852 (1975).
9. C. W. HIRT, Los Alamos Report LA-UR-78-2813 (1978).
10. Y. YAMASHITA, K. SAKAI, AND H. HISHIDA, *Trans. At. Energy Soc. Japan* (Mar. 1979), C54.
11. K. SAKAI, H. HISHIDA, AND Y. YAMASHITA, *Nucl. Eng. Des.*, in press.
12. S. P. FRANKEL, "Math Tables and Other Aids to Computation," **4** (1950), 65.

RECEIVED: September 18, 1979

KATSUHIRO SAKAI

*Mitsubishi Atomic Power Industries, Inc.
Nuclear Development Center
1-297 Kitabukuro-Cho
Omiya City, Saitama Prefecture
Japan*